Supplementary Information:

Self-selective passivation of the diversely charged $SnO_2/CsPbI_3$ heterointerfaces by binary ionic compound

Huiwen Xiang,[1] Jinping Zhang,[2] Ke Zhao,[3] Haiyue Zhang,[1] Feifei Ren,[1] Yu Jia,[1] Chengyan Liu,[1, 2*]

[1]Henan Key Laboratory of Photovoltaic Materials, Key Laboratory for Special Functional Materials of Ministry of Education, and School of Materials Science and Engineering, Henan University, Kaifeng 475004, China.

[2]Faculty of Engineering, Huanghe Science and Technology College, Zhengzhou 450006, China

[3]International Laboratory for Quantum Functional Materials of Henan, and School of Physics and Microelectronics, Zhengzhou University, Zhengzhou 450001, China

*Electronic mail: cyliu@henu.edu.cn

I. Atomic structures and surface energy calculations

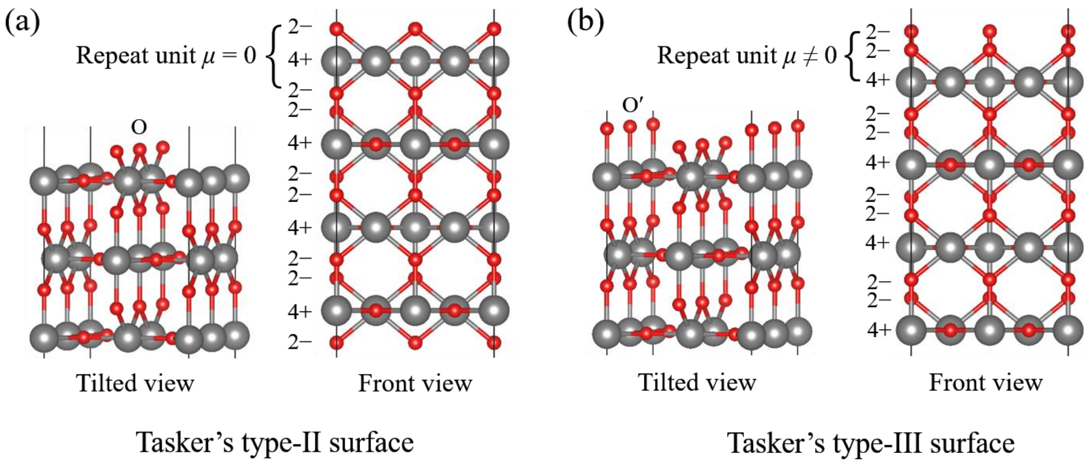

Fig. S1. The O-terminated and O′-terminated SnO_2 surfaces. (a) The O-terminated SnO_2 surface that is stable Tasker's type-II surface with charged planes but no net dipole moment (μ) perpendicular to surface. (b) The O′-terminated SnO_2 surface that is unstable Tasker's type-III surface with dipole moment normal to surface.

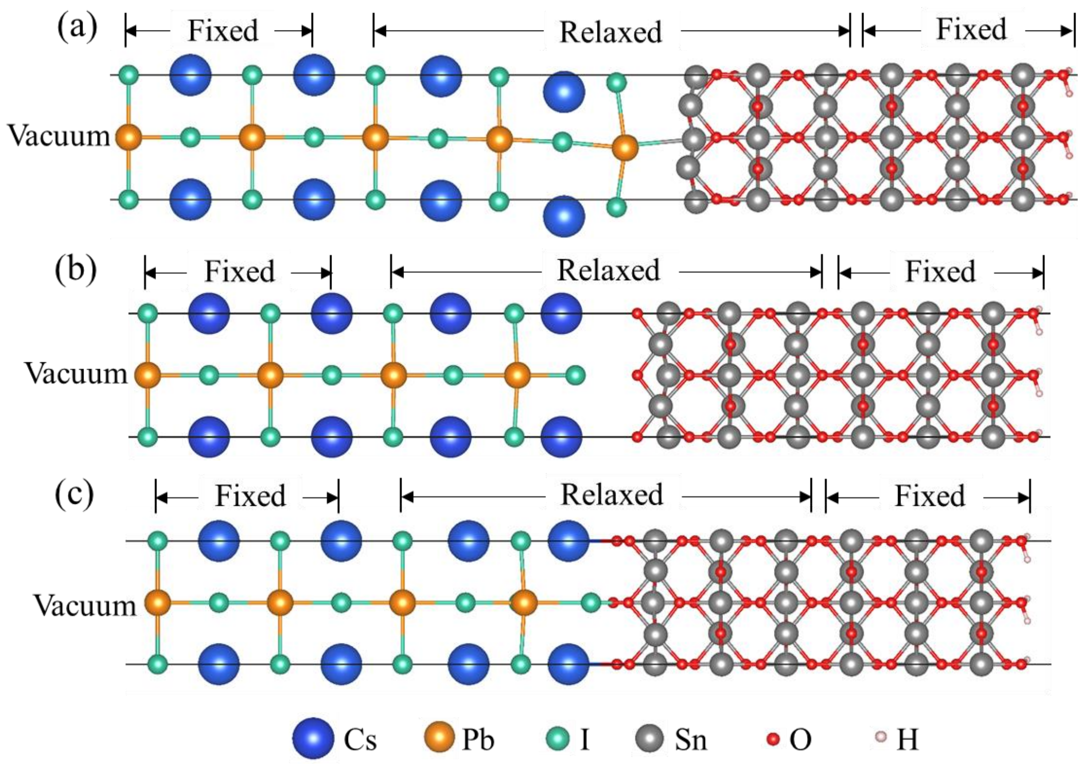

Fig. S2. The relaxed atomic structures of SnO_2 (110)/$CsPbI_3$ (100) heterojunctions with relatively higher binding energies than that of structures shown by Fig. 1 in the main text. (a) The slab of SnO_2-SnO/$CsPbI_3$-PbI heterojunction with SnO-terminal of SnO_2 (110) and PbI-terminal of $CsPbI_3$ (100) interfaces. (b) The slab of SnO_2-O/$CsPbI_3$-CsI heterojunction with O-terminal of SnO_2 (110) and CsI-terminal of $CsPbI_3$ (100) interfaces. (c) The slab of SnO_2-O′/$CsPbI_3$-CsI heterojunction with O′-terminal of SnO_2 (110) and CsI-terminal of $CsPbI_3$ (100) interfaces. The lattice constants of the slab are a = 6.43 Å, b = 6.58 Å and c =72.00 Å with a 20 Å vacuum layer. The atoms colored blue, gold, green, grey, red and pink represent Cs, Pb, I, Sn, O and pseudo-H, respectively. The relaxed and fixed atomic layers represent the interface and the bulk, respectively.

The surface energies of SnO_2 (110) and $CsPbI_3$ (100) are calculated based on the models shown in Fig. S3. The calculation formulas are

$$E_{\mathrm{A}}(\mathrm{surface}) = \frac{1}{2}[E_{\mathrm{A\text{-}slab}} - 8E_{\mathrm{A}} - 4(\mu_{\mathrm{O}} + \mu_{\mathrm{O}}^{0})] \quad (\mathrm{S1})$$

and

$$E_{\mathrm{B}}(\mathrm{surface}) = \frac{1}{2}[E_{\mathrm{B\text{-}slab}} - 4E_{\mathrm{B}} - (\mu_{\mathrm{Pb}} + \mu_{\mathrm{Pb}}^{0}) - 2(\mu_{\mathrm{I}} + \mu_{\mathrm{I}}^{0})] \quad (\mathrm{S2})$$

where E_{A} (surface) and E_{B} (surface) are surface energies of SnO_2 and $CsPbI_3$, respectively. $E_{\mathrm{A(B)\text{-}slab}}$ and $E_{\mathrm{A(B)}}$ are the total energies of the SnO_2 ($CsPbI_3$) slab [Fig. S3b(d)] and SnO_2 ($CsPbI_3$) primitive cell [Fig. 3a(c)], respectively. μ_{O}, μ_{Pb} and μ_{I} are the chemical potentials of O, Pb and I atoms relative to those of their pure elemental phases μ_{O}^{0}, μ_{Pb}^{0} and μ_{I}^{0}, respectively. Under equilibrium growth condition, the elemental chemical potentials of SnO_2 are restricted by $\mu_{\mathrm{Sn}} + 2\mu_{\mathrm{O}} = \Delta H_{\mathrm{SnO_2}}$,

$\mu_{Sn} \leq 0$ and $\mu_{O} \leq 0$, while the elemental chemical potentials of $CsPbI_3$ are referenced to the calculations in Ref. S1.

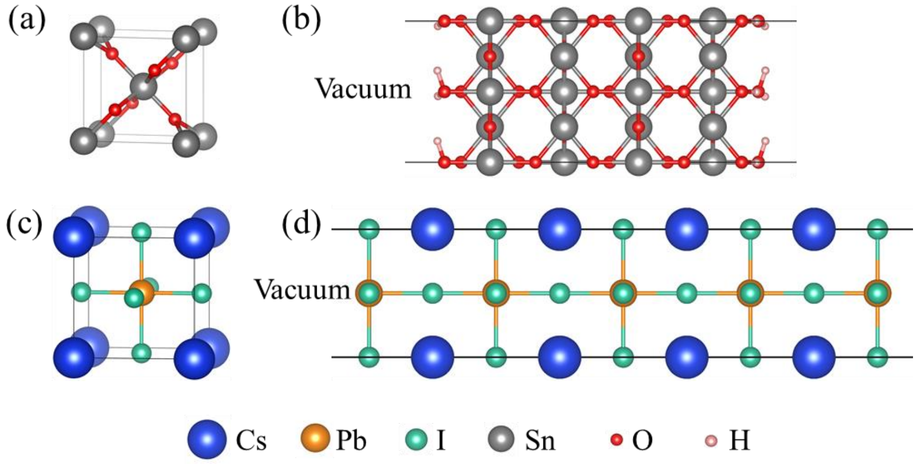

Fig. S3. The primitive cell and slab model of tetragonal SnO_2 and cubic $CsPbI_3$. (a) Primitive cell of tetragonal SnO_2 with a space group of $P4_2/mnm$. (b) SnO_2 (1 1 0) slab with O-terminal surfaces whose dangling bonds are passivated by pseudo-hydrogen of H.66 pseudopotential. The slab consists of 16 Sn atoms, 36 O atoms, 12 pseudo-H atoms and a 30 Å vacuum layer. (c) Primitive cell of cubic $CsPbI_3$ with a space group of $Pm\bar{3}m$. (d) $CsPbI_3$ (1 0 0) slab with PbI-terminal surfaces. The slab consists of 4 Cs atoms, 5 Pb atoms, 14 I atoms and a 20 Å vacuum layer. The atoms colored blue, gold, cyan, grey, red and pink represent Cs, Pb, I, Sn, O and pseudo-H, respectively.

II. Elemental chemical potentials for SnO_2 phase

To obtain the SnO_2 host in thermodynamic equilibrium conditions, the chemical potentials of Sn and O should satisfy

$$\mu_{Sn} + 2\mu_{O} = \Delta H_{SnO_2} \ (-4.96 \text{ eV}) \qquad \text{(S3)}$$

where μ_{Sn} and μ_{O} are the chemical potentials of Sn and O, respectively, referenced to their most stable pure phases, and ΔH_{SnO_2} is the formation enthalpy of SnO_2. In addition, the precipitation of the elemental host should be avoided by

$$\mu_{Sn} \leq 0, \ \ \mu_{O} \leq 0 \qquad \text{(S4)}$$

Considering the Mg, Zn, N and Cl dopants incorporation with the maximum allowed chemical potentials, the associated secondary phases between these dopants and the host elements need to be excluded by the conditions as determined by inequalities (S5), (S6), (S7) and (S8) for Mg, Zn, N and Cl dopants, respectively. Based on this, the maximum allowed chemical potentials of dopants in SnO_2 phase diagram are restricted by the secondary phases of Mg_2SnO_4 and ZnO under Mg and Zn cations doping, and by $SnCl_2$, $SnCl_4$ and $Sn(NO_3)_4$ under Cl and N anions doping (Fig. 3a and 3b of the main text).

$$\begin{cases} 9\mu_{Mg} + 5\mu_{Sn} \le \Delta H_{Mg_9Sn_5\ (R3)}\left(-2.57\ eV\right) & \mu_{Mg} + 2\mu_{Sn} + 5\mu_{O} \le \Delta H_{MgSn_2O_5\,(Cmcm)}\left(-15.27\ eV\right) \\ 2\mu_{Mg} + \mu_{Sn} \le \Delta H_{Mg_2Sn\ (Fm\bar{3}m)}\left(-0.57\ eV\right) & 2\mu_{Mg} + 3\mu_{Sn} + 8\mu_{O} \le \Delta H_{Mg_2Sn_3O_8\,(P6_3mc)}\left(-25.48\ eV\right) \\ 3\mu_{Mg} + \mu_{Sn} \le \Delta H_{Mg_3Sn\ (Pm\bar{3}m)}\left(-0.56\ eV\right) & 3\mu_{Mg} + 2\mu_{Sn} + 7\mu_{O} \le \Delta H_{Mg_3Sn_2O_7\,(Cmc2_1)}\left(-25.84\ eV\right) \\ \mu_{Mg} + \mu_{Sn} \le \Delta H_{MgSn\ (P4/mmm)}\left(-0.25\ eV\right) & 2\mu_{Mg} + 9\mu_{Sn} + 13\mu_{O} \le \Delta H_{Mg_2Sn_9O_{13}\,(C2/m)}\left(-37.48\ eV\right) \\ \mu_{Mg} + 3\mu_{Sn} \le \Delta H_{MgSn_3\ (P6_3/mmc)}\left(-0.08\ eV\right) & \mu_{Mg} + 2\mu_{Sn} + 4\mu_{O} \le \Delta H_{Mg(SnO_2)_2\ (Imma)}\left(-12.38\ eV\right) \\ \mu_{Mg} + 2\mu_{Sn} \le \Delta H_{MgSn_2\ (C2/c)}\left(-0.15\ eV\right) & \mu_{Mg} + 4\mu_{Sn} + 8\mu_{O} \le \Delta H_{Mg(SnO_2)_4\ (Cm)}\left(-21.27\ eV\right) \\ \mu_{Mg} + 5\mu_{Sn} \le \Delta H_{MgSn_5\ (P\bar{6}2m)}\left(-0.12\ eV\right) & \mu_{Mg} + \mu_{Sn} + 2\mu_{O} \le \Delta H_{MgSnO_2\ (P\bar{1})}\left(-7.38\ eV\right) \\ 5\mu_{Mg} + \mu_{Sn} \le \Delta H_{Mg_5Sn\ (R32)}\left(-0.32\ eV\right) & \mu_{Mg} + 4\mu_{Sn} + 9\mu_{O} \le \Delta H_{MgSn_4O_9\ (P4/n)}\left(-22.82\ eV\right) \\ \mu_{Mg} + \mu_{O} \le \Delta H_{MgO\ (Fm\bar{3}m)}\left(-5.49\ eV\right) & \mu_{Mg} + 3\mu_{Sn} + 7\mu_{O} \le \Delta H_{MgSn_3O_7\ (Pnma)}\left(-18.22\ eV\right) \\ \mu_{Mg} + 2\mu_{O} \le \Delta H_{MgO_2\ (Pa\bar{3})}\left(-5.19\ eV\right) & 2\mu_{Mg} + 2\mu_{Sn} + 5\mu_{O} \le \Delta H_{Mg_2Sn_2O_5\ (Pbam)}\left(-14.93\ eV\right) \\ 2\mu_{Mg} + \mu_{Sn} + 4\mu_{O} \le \Delta H_{Mg_2SnO_4\,(Imma)}\left(-16.11\ eV\right) & \mu_{Mg} + \mu_{Sn} + 6\mu_{O} \le \Delta H_{MgSnO_6\ (Fm\bar{3}m)}\left(-0.99\ eV\right) \\ \mu_{Mg} + \mu_{Sn} + 3\mu_{O} \le \Delta H_{MgSnO_3\,(R\bar{3})}\left(-10.52\ eV\right) & \end{cases} \quad (S5)$$

$$\begin{cases} 3\mu_{Zn} + \mu_{Sn} \le \Delta H_{Zn_3Sn\ (P\bar{1})}\left(0.33\ eV\right) & \mu_{Zn} + \mu_{Sn} + 2\mu_{O} \le \Delta H_{ZnSnO_2\,(P\bar{1})}\left(-5.13\ eV\right) \\ \mu_{Zn} + 3\mu_{Sn} \le \Delta H_{ZnSn_3\,(P6_3/mmc)}\left(0.48\ eV\right) & \mu_{Zn} + 2\mu_{Sn} + 4\mu_{O} \le \Delta H_{Zn(SnO_2)_2\,(Imma)}\left(-9.61\ eV\right) \\ \mu_{Zn} + \mu_{O} \le \Delta H_{ZnO(P6_3mc)}\left(-2.90\ eV\right) & \mu_{Zn} + 4\mu_{Sn} + 8\mu_{O} \le \Delta H_{Zn(SnO_2)_4\,(Cm)}\left(-18.81\ eV\right) \\ \mu_{Zn} + 2\mu_{O} \le \Delta H_{ZnO_2\,(Pa\bar{3})}\left(-2.23\ eV\right) & 2\mu_{Zn} + 9\mu_{Sn} + 13\mu_{O} \le \Delta H_{Zn_2Sn_9O_{13}\,(P\bar{1})}\left(-31.37\ eV\right) \\ 2\mu_{Zn} + \mu_{Sn} + 4\mu_{O} \le \Delta H_{Zn_2SnO_4\,(Imma)}\left(-10.64\ eV\right) & \mu_{Zn} + 3\mu_{Sn} + 7\mu_{O} \le \Delta H_{ZnSn_3O_7\,(Pnma)}\left(-15.19\ eV\right) \\ \mu_{Zn} + \mu_{Sn} + 3\mu_{O} \le \Delta H_{ZnSnO_3\,(R3c)}\left(-7.66\ eV\right) & \mu_{Zn} + 4\mu_{Sn} + 9\mu_{O} \le \Delta H_{ZnSn_4O_9\,(P4/n)}\left(-19.75\ eV\right) \\ \mu_{Zn} + 2\mu_{Sn} + 5\mu_{O} \le \Delta H_{ZnSn_2O_5\,(Cmcm)}\left(-12.33\ eV\right) & \mu_{Zn} + 5\mu_{Sn} + 7\mu_{O} \le \Delta H_{ZnSn_5O_7\,(Cmcm)}\left(-14.73\ eV\right) \\ 3\mu_{Zn} + 2\mu_{Sn} + 7\mu_{O} \le \Delta H_{Zn_3Sn_2O_7\,(Cmc2_1)}\left(-17.86\ eV\right) & 2\mu_{Zn} + 2\mu_{Sn} + 5\mu_{O} \le \Delta H_{Zn_2Sn_2O_5\,(Pmc2_1)}\left(-11.50\ eV\right) \\ 2\mu_{Zn} + 3\mu_{Sn} + 8\mu_{O} \le \Delta H_{Zn_2Sn_3O_8\,(P6_3mc)}\left(-19.64\ eV\right) & \mu_{Zn} + 4\mu_{Sn} + 6\mu_{O} \le \Delta H_{Zn(Sn_2O_3)_2\,(Cmcm)}\left(-11.89\ eV\right) \end{cases} \quad (S6)$$

$$\begin{cases} 3\mu_{Sn} + 4\mu_{N} \le \Delta H_{Sn_3N_4\ (Fd\bar{3}m)}\left(1.47\ eV\right) & 2\mu_{N} + \mu_{O} \le \Delta H_{N_2O\,(P2_13)}\left(-0.15\ eV\right) \\ \mu_{Sn} + \mu_{N} \le \Delta H_{SnN\,(Cm)}\left(0.94\ eV\right) & \mu_{N} + 2\mu_{O} \le \Delta H_{NO_2\ (P2_1/c)}\left(-0.13\ eV\right) \\ 3\mu_{Sn} + \mu_{N} \le \Delta H_{Sn_3N\,(P6_3/mmc)}\left(-4.02\ eV\right) & \mu_{N} + 3\mu_{O} \le \Delta H_{NO_3\ (P2_1/c)}\left(-0.05\ eV\right) \\ \mu_{Sn} + 4\mu_{N} + 12\mu_{O} \le \Delta H_{Sn(NO_3)_4\ (P2_1/c)}\left(-8.01\ eV\right) & 2\mu_{N} + 3\mu_{O} \le \Delta H_{N_2O_3\ (P2_12_12_1)}\left(-0.14\ eV\right) \\ 2\mu_{Sn} + 2\mu_{N} + \mu_{O} \le \Delta H_{Sn_2N_2O\,(I4_1/amd)}\left(-1.64\ eV\right) & \mu_{N} + \mu_{O} \le \Delta H_{NO\,(P2_12_12_1)}\left(1.29\ eV\right) \\ 2\mu_{N} + 5\mu_{O} \le \Delta H_{N_2O_5\ (P6_3/mmc)}\left(-1.01\ eV\right) & \end{cases}$$

(S7)

$$\begin{cases} \mu_{Sn} + \mu_{Cl} \le \Delta H_{SnCl\,(P6_3mc)}\left(-1.08\ eV\right) & 2\mu_{Cl} + 7\mu_{O} \le \Delta H_{Cl_2O_7\ (C2/c)}\left(1.46\ eV\right) \\ \mu_{Sn} + 2\mu_{Cl} \le \Delta H_{SnCl_2\ (Pnma)}\left(-3.56\ eV\right) & 2\mu_{Cl} + \mu_{O} \le \Delta H_{Cl_2O\,(I4_1/amd)}\left(0.34\ eV\right) \\ \mu_{Sn} + 4\mu_{Cl} \le \Delta H_{SnCl_4\ (P2_1/c)}\left(-4.33\ eV\right) & \mu_{Cl} + 2\mu_{O} \le \Delta H_{ClO_2\ (pbca)}\left(0.76\ eV\right) \\ 2\mu_{Sn} + 4\mu_{Cl} + 3\mu_{O} \le \Delta H_{Sn_2Cl_4O_3\ (P2_1/c)}\left(-7.34\ eV\right) & \mu_{Cl} + 3\mu_{O} \le \Delta H_{ClO_3\ (Cc)}\left(0.32\ eV\right) \\ \mu_{Sn} + 3\mu_{Cl} + 4\mu_{O} \le \Delta H_{SnCl_3O_4\ (P2_1/c)}\left(-3.21\ eV\right) & \mu_{Cl} + 5\mu_{O} \le \Delta H_{ClO_5\ (P2_1/c)}\left(1.75\ eV\right) \\ \mu_{Sn} + 4\mu_{Cl} + 5\mu_{O} \le \Delta H_{SnCl_4O_5\ (C2/c)}\left(-1.32\ eV\right) & \mu_{Cl} + 6\mu_{O} \le \Delta H_{ClO_6\ (Pnma)}\left(2.08\ eV\right) \\ \mu_{Sn} + 2\mu_{Cl} + 2\mu_{O} \le \Delta H_{Sn(ClO)_2\ (P2_1/c)}\left(-2.25\ eV\right) & \mu_{Cl} + \mu_{O} \le \Delta H_{ClO\,(Pm\bar{3}m)}\left(0.53\ eV\right) \end{cases} \quad (S8)$$

III. Electronic structures of the energetically favorable interfaces

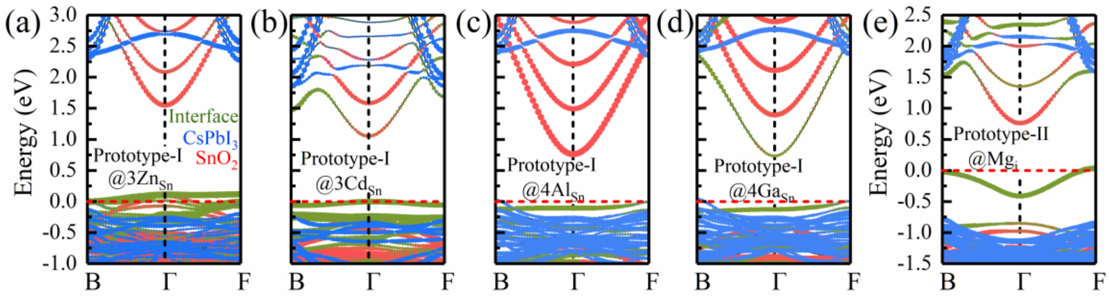

Fig. S4. Band structures of the prototype-I heterojunction with defects of (a) $3Zn_{Sn}$, (b) $3Cd_{Sn}$, (c) $4Al_{Sn}$ and (d) $4Ga_{Sn}$ at the interface, and (e) the prototype-II heterojunction with defects of Mg_i. The red, blue and green circles in the band structures represent the contribution of the electronic states that come from the bulk SnO_2, $CsPbI_3$ and the interface, respectively. The red dashed lines indicate the energy positions of the highest occupied states.

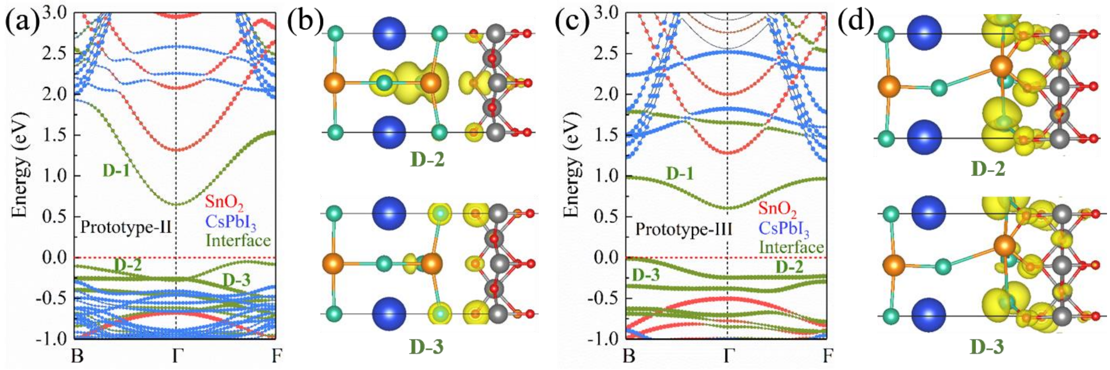

Fig. S5. Band structure and interfacial structure with partial charge densities of prototype-II and prototype-III heterojunctions. (a) Band structures of the prototype-II heterojunction. The interfacial charge distribution in real space corresponding to the interfacial states D-2 and D-3 are displayed in (b). (c) Band structures of the prototype-III heterojunction. The interfacial charge distribution in real space corresponding to the interfacial states D-2 and D-3 are shown in (d).

IV. Nonadiabatic molecular dynamics (NAMD) simulations

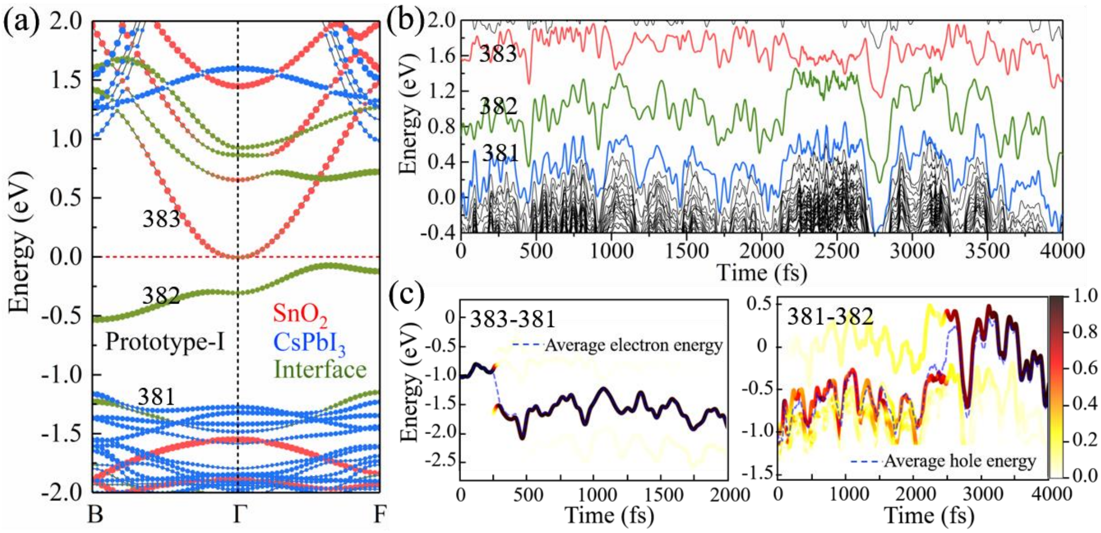

Fig. S6. Band structure, time-dependent evolutions of the energy states and time-dependent energy for carrier trapping of the Prototype-I heterojunction. (a) Band structure of prototype-I heterojunction. The red, blue and green circles in the band structures represent the contribution of the electronic states from the bulk SnO_2, $CsPbI_3$ and the interface, respectively. The representations are remained in the following figures of band structure. (b) Time-dependent evolutions of the energy states of prototype-I heterojunction with a time step of 0.5 fs. (c) Time-dependent energy change for electron and hole trapping of the prototype-I heterojunction. The color strip indicates the electron or hole distribution on different energy states, and the blue dashed line represents the averaged electron (left) or hole (right) energy. The electron and hole trapping paths are from the band index 383 to 381 (trapped at band index 382) and from the band index 381 to 382, respectively.

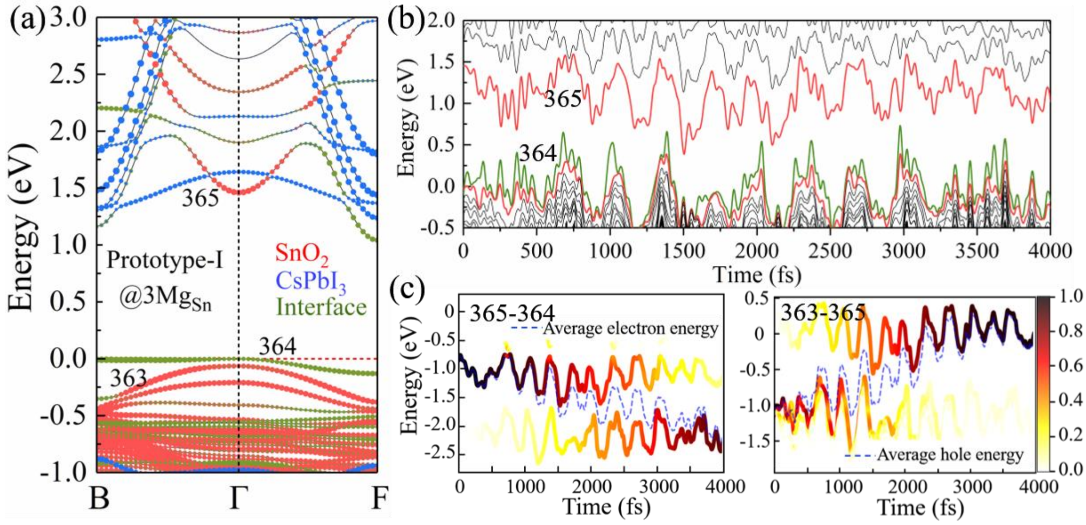

Fig. S7. Band structure, time-dependent evolutions of the energy states and time-dependent energy for carrier trapping of the prototype-I heterojunction with $3Mg_{Sn}$ defect at the interface. (a) Band structure of $3Mg_{Sn}$-doped prototype-I heterojunction. (b) Time-dependent evolutions of the energy states of $3Mg_{Sn}$-doped prototype-I heterojunction with a time step of 0.5 fs. (c) Time-dependent energy change for electron and hole trapping of the

$3Mg_{Sn}$-doped prototype-I heterojunction. The color strip indicates the electron or hole distribution on different energy states, and the blue dashed line represents the averaged electron (left) or hole (right) energy. The electron and hole trapping paths are from band index 365 to 364 and from band index 363 to 365, respectively.

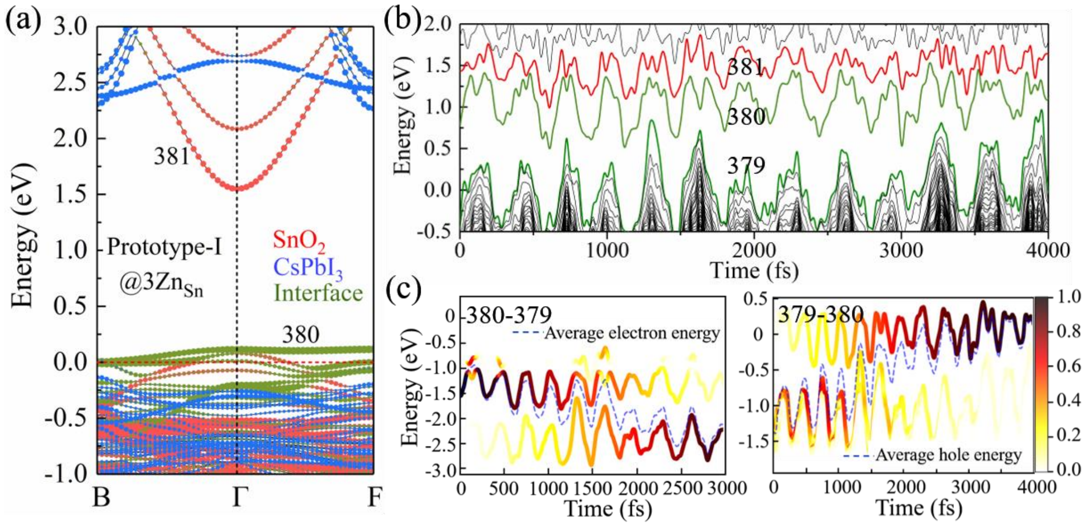

Fig. S8. Band structure, time-dependent evolutions of the energy states and time-dependent energy for carrier trapping of the prototype-I heterojunction with $3Zn_{Sn}$ defect at the interface. (a) Band structure of $3Zn_{Sn}$-doped prototype-I heterojunction. (b) Time-dependent evolutions of the energy states of $3Zn_{Sn}$-doped prototype-I heterojunction with a time step of 0.5 fs. (c) Time-dependent energy change for electron and hole trapping of the $3Zn_{Sn}$-doped prototype-I heterojunction. The color strip indicates the electron or hole distribution on different energy states, and the blue dashed line represents the averaged electron (left) or hole (right) energy. The electron and hole trapping paths are from band index 380 to 379 and from band index 379 to 380, respectively.

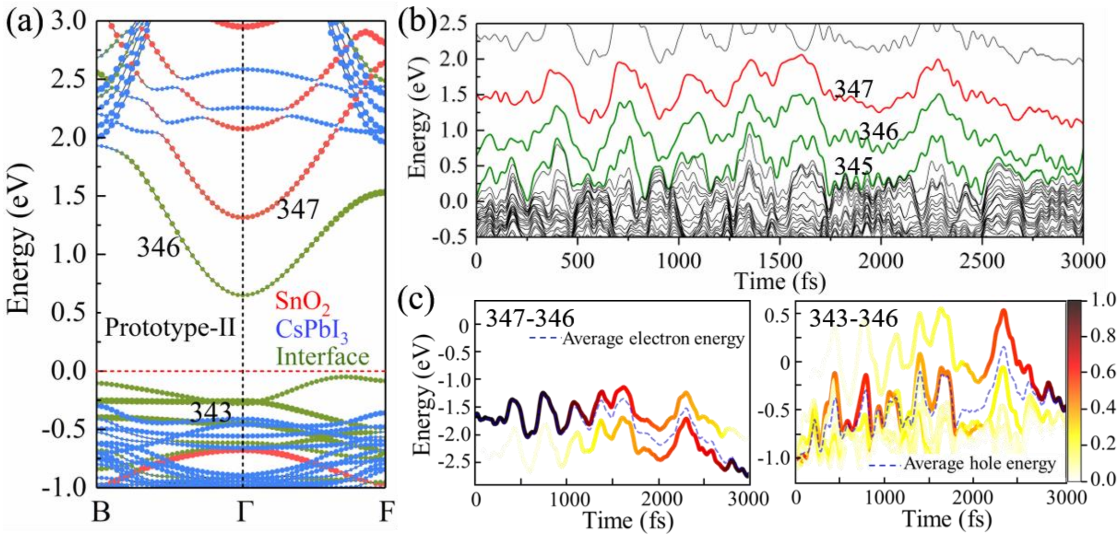

Fig. S9. Band structure, time-dependent evolutions of the energy states and time-dependent energy for carrier trapping of the prototype-II heterojunction. (a) Band structure of prototype-II heterojunction. (b) Time-dependent evolutions of the energy states of prototype-II heterojunction with a time step of 0.5 fs. (c) Time-dependent energy change for electron and hole trapping of the prototype-II heterojunction. The color strip indicates the electron or hole distribution on different energy states, and the blue dashed line represents the averaged electron (left) or hole (right) energy. The electron and hole trapping paths are from band index 347 to 346 and from band index 343 to 346, respectively.

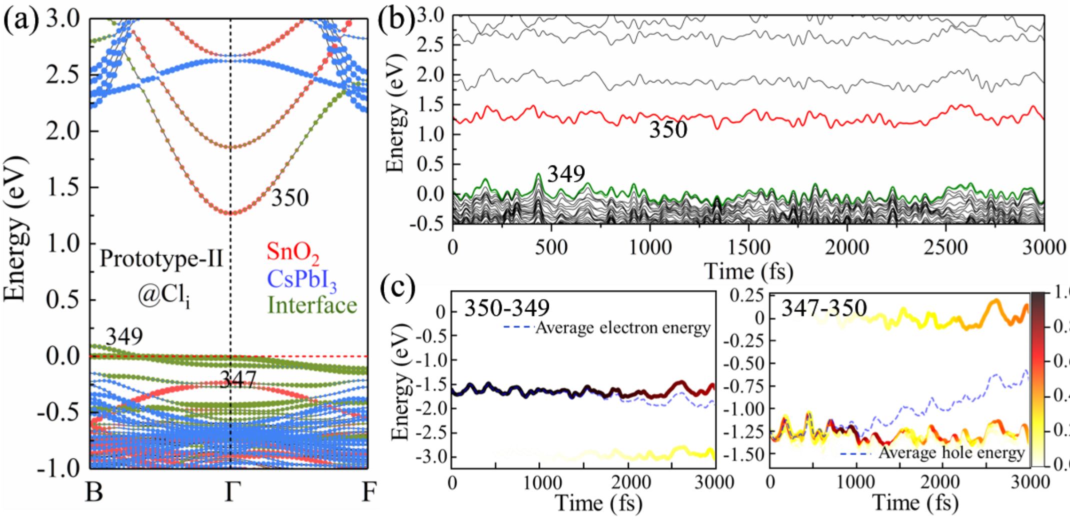

Fig. S10. Band structure, time-dependent evolutions of the energy states and time-dependent energy for carrier trapping of the prototype-II heterojunction with Cl_i defect at the interface. (a) Band structure of Cl_i -doped prototype-II heterojunction. (b) Time-dependent evolutions of the energy states of Cl_i -doped prototype-II heterojunction with a time step of 0.5 fs. (c) Time-dependent energy change for electron and hole trapping of the Cl_i-doped prototype-II heterojunction. The color strip indicates the electron or hole distribution on different energy states, and the blue dashed line represents the averaged electron (left) or hole (right) energy. The electron and hole trapping paths are from band index 350 to 349 and from band index 347 to 350, respectively.

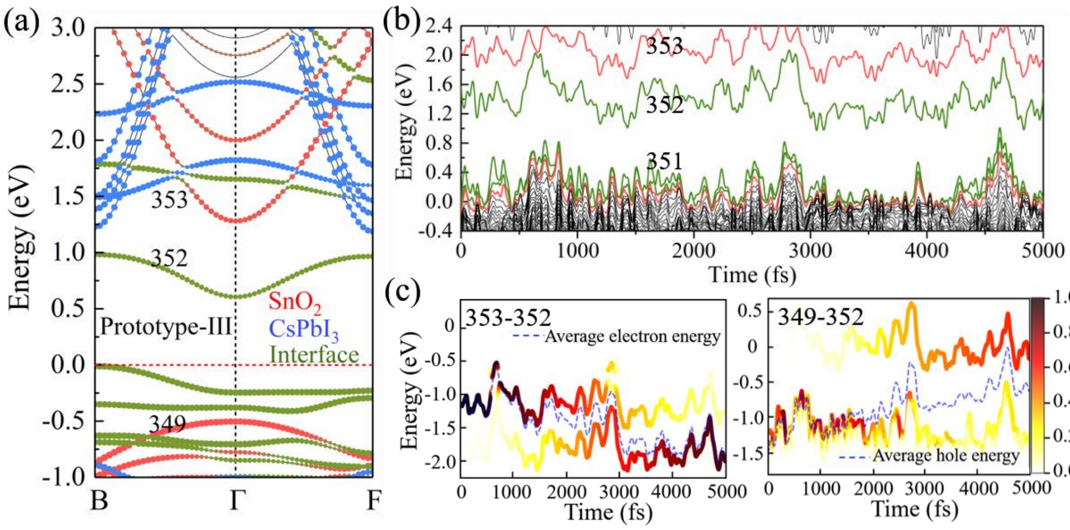

Fig. S11. Band structure, time-dependent evolutions of the energy states and time-dependent energy for carrier trapping of the prototype-III heterojunction. (a) Band structure of prototype-III heterojunction. (b) Time-dependent evolutions of the energy states of prototype-III heterojunction with a time step of 0.5 fs. (c) Time-dependent energy change for electron and hole trapping of the prototype-III heterojunction. The color strip indicates the electron or hole distribution on different energy states, and the blue dashed line represents the averaged electron (left) or hole (right) energy. The electron and hole trapping paths are from band index 353 to 352 and from band index 349 to 352, respectively.

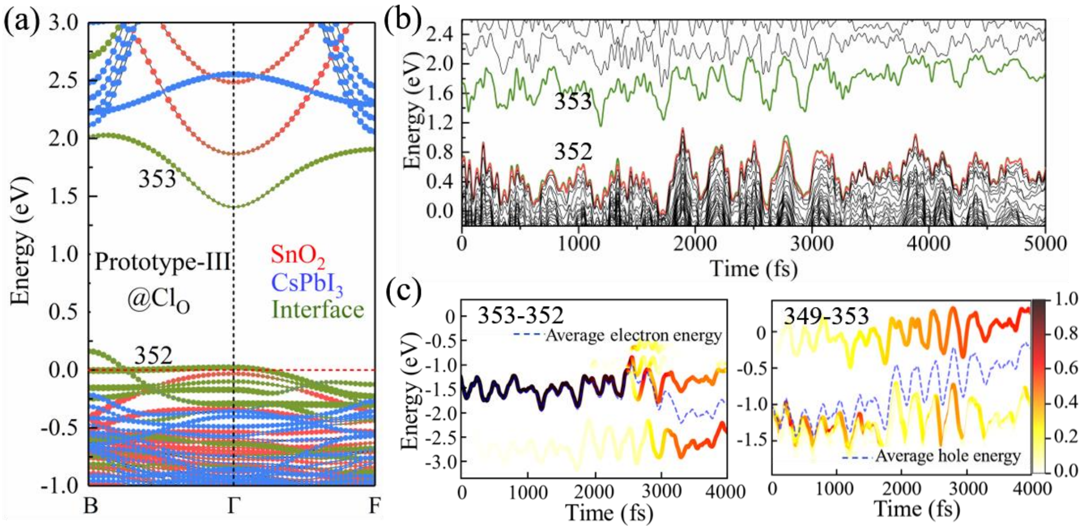

Fig. S12. Band structure, time-dependent evolutions of the energy states and time-dependent energy for carrier trapping of the prototype-III heterojunction with Cl_O defect at the interface. (a) Band structure of Cl_O-doped prototype-III heterojunction. (b) Time-dependent evolutions of the energy states of Cl_O-doped prototype-III heterojunction with a time step of 0.5 fs. (c) Time-dependent energy change for electron and hole trapping of the Cl_O-doped prototype-III heterojunction. The color strip indicates the electron or hole distribution on different energy states, and the blue dashed line represents the averaged electron (left) or hole (right) energy. The electron and hole trapping paths are from band index 353 to 352 and from band index 349 to 353, respectively.

Reference:

S1 Y. Huang, W.-J. Yin, and Y. He, *J. Phys. Chem. C*, 2018, 122(2), 1345–1350.

Appendix:

1. POSCAR of the prototype-I heterojunction

```
System
   1.00000000000000
     6.4278000000000004    0.0000000000000000    0.0000000000000000
     0.0000000000000000    6.5816000000000008    0.0000000000000000
     0.0000000000000000    0.0000000000000000   71.5254999999999939
   Sn    O    Cs    Pb    I    H
   24    48    4    4    12    6
Direct
  0.9999919999999989  0.5000000000000000  0.3658322055490686
  0.9999919999999989  0.0000000000000000  0.4132032055490740
  0.9999919999999989  0.5000000000000000  0.4605752055490697
  0.9999980271187141  0.0013979567503384  0.5088902585905188
  0.0000038882491324  0.4991704104496293  0.5554638207358735
```

154	0.9999845672805776	0.0030765047559100	0.6090991386037246
155	0.7499919999999989	0.0000000000000000	0.3658322055490686
156	0.7499919999999989	0.5000000000000000	0.4132032055490740
157	0.7499919999999989	0.0000000000000000	0.4605752055490697
158	0.7501860797163218	0.5003890284283088	0.5077432971924054
159	0.7509098087503929	0.9981980800859063	0.5572865927069941
160	0.7524938036872300	0.5047714573209348	0.6022919793327901
161	0.4999919999999989	0.5000000000000000	0.3658322055490686
162	0.4999919999999989	0.0000000000000000	0.4132032055490740
163	0.4999919999999989	0.5000000000000000	0.4605752055490697
164	0.4999974077579381	0.0011334690122879	0.5088526002566667
165	0.5000040667617398	0.5001768191365201	0.5548621393110906
166	0.5000214049225065	0.9935002142624114	0.6044360549686658
167	0.2499919999999989	0.0000000000000000	0.3658322055490686
168	0.2499919999999989	0.5000000000000000	0.4132032055490740
169	0.2499919999999989	0.0000000000000000	0.4605752055490697
170	0.2498073652516979	0.5003913661843029	0.5077435943818003
171	0.2490972409506966	0.9981945619816059	0.5572876627383607
172	0.2475598864684230	0.5047878616561050	0.6022918531468093
173	0.9999919999999989	0.1938200000000023	0.3658322055490686
174	0.9999919999999989	0.6938200000000023	0.4132032055490669
175	0.9999919999999989	0.1938200000000023	0.4605752055490697
176	0.9999956447081502	0.6943942599486448	0.5091771205980322
177	0.0000058686565083	0.1944806343048242	0.5585248801419596
178	0.0000197880216817	0.6586511602206997	0.6145178165379832
179	0.9999919999999989	0.8061800000000048	0.3658322055490686
180	0.9999919999999989	0.3061799999999977	0.4132032055490669
181	0.9999919999999989	0.8061800000000048	0.4605752055490697
182	0.9999974342640314	0.3075954915188532	0.5079549097542326
183	0.0000038584746633	0.8052370456751206	0.5555495942408442
184	0.0000335599725503	0.3104347963407861	0.5993225735383021
185	0.7499919999999989	0.5000000000000000	0.3474692055490678
186	0.7499919999999989	0.0000000000000000	0.3948412055490707
187	0.7499919999999989	0.5000000000000000	0.4422122055490689
188	0.7498108008237097	0.9969907957804480	0.4901955915975833
189	0.7512183518468305	0.4884913854842878	0.5372050413003677
190	0.7572340621318219	0.9615732296179971	0.5872298885354041
191	0.7499919999999989	0.0000000000000000	0.3368232055490665
192	0.7499919999999989	0.5000000000000000	0.3841942055490719
193	0.7499919999999989	0.0000000000000000	0.4315662055490677
194	0.7499919999999989	0.5000000000000000	0.4789372055490730
195	0.7496936590770318	0.0092541149831646	0.5279252535854440
196	0.7461310318512204	0.5206773703828489	0.5741319956220963
197	0.4999919999999989	0.1938200000000023	0.3658322055490686

198	0.4999919999999989	0.6938200000000023	0.4132032055490669
199	0.4999919999999989	0.1938200000000023	0.4605752055490697
200	0.4999977317086532	0.6939166067180409	0.5094451661110497
201	0.5000005324647461	0.1950266979997579	0.5598570660142812
202	0.5000292517566223	0.6842396218947684	0.6110712385155566
203	0.4999919999999989	0.8061800000000048	0.3658322055490686
204	0.4999919999999989	0.3061799999999977	0.4132032055490669
205	0.4999919999999989	0.8061800000000048	0.4605752055490697
206	0.4999962161713682	0.3078085217042243	0.5082378878767173
207	0.5000035489693744	0.8073931929046623	0.5556855571608992
208	0.5000181101873693	0.3094035105363560	0.6069153269041294
209	0.2499919999999989	0.5000000000000000	0.3474692055490678
210	0.2499919999999989	0.0000000000000000	0.3948412055490707
211	0.2499919999999989	0.5000000000000000	0.4422122055490689
212	0.2501816297971047	0.9969886855907575	0.4901958872918541
213	0.2487847539683798	0.4884932395404675	0.5372048996087742
214	0.2427759639281746	0.9615606516204025	0.5872328348824780
215	0.2499919999999989	0.0000000000000000	0.3368232055490665
216	0.2499919999999989	0.5000000000000000	0.3841942055490719
217	0.2499919999999989	0.0000000000000000	0.4315662055490677
218	0.2499919999999989	0.5000000000000000	0.4789372055490730
219	0.2503043358733805	0.0092533040148339	0.5279255522642075
220	0.2538849079540100	0.5206877561036549	0.5741316769618621
221	0.0001185901474372	0.5151603543752898	0.6646454579208623
222	0.9999378304400750	0.4995661667786138	0.7456720677369688
223	0.0000000000000000	0.4999970000000005	0.8274090000000029
224	0.0000000000000000	0.4999970000000005	0.9166999999999987
225	0.4999190609860804	0.0055337705667071	0.6958872134457579
226	0.4999778477366021	0.0001229477859610	0.7837747929188836
227	0.5000000000000000	0.9999970000000005	0.8720550000000031
228	0.5000000000000000	0.9999970000000005	0.9613470000000035
229	0.9999247186035731	0.0046019710103451	0.6979668191930699
230	0.9999800075912546	0.9999450224720690	0.7841702612090771
231	0.0000000000000000	0.9999970000000005	0.8720550000000031
232	0.0000000000000000	0.9999970000000005	0.9613470000000035
233	0.5000163062447953	0.5039643607200048	0.6987131867308278
234	0.4999773689709812	0.5001027642756881	0.7843106955225565
235	0.5000000000000000	0.4999970000000005	0.8720550000000031
236	0.5000000000000000	0.4999970000000005	0.9613470000000035
237	0.4996272617681328	0.0180199509342458	0.6530886933850653
238	0.4999688145967056	0.0010663402596833	0.7407567871083458
239	0.5000000000000000	0.9999970000000005	0.8274090000000029
240	0.5000000000000000	0.9999970000000005	0.9166999999999987
241	0.7145289999999989	0.8547900000000013	0.3326282055490708

```
0.3989049999999992  0.0328710000000001  0.3323232055490735
0.2186459999999997  0.8537740000000014  0.3326462055490680
0.2471290000000010  0.3833580000000012  0.3378912055490702
0.8997850000000014  0.0292540000000017  0.3323302055490700
0.7470209999999966  0.3828060000000022  0.3379422055490693
```

2. POSCAR of the prototype-II heterojunction

```
System
   1.00000000000000
     6.4278000000000004    0.0000000000000000    0.0000000000000000
     0.0000000000000000    6.5816000000000008    0.0000000000000000
     0.0000000000000000    0.0000000000000000   66.0000000000000000
   Sn   O   Cs   Pb   I   H
   20   42   4    5    14   6
Selective dynamics
Direct
  0.2500000000000000  0.5000000000000000  0.1575786969696935
  0.2500000000000000  0.0000000000000000  0.2089156969696973
  0.2500000000000000  0.5000000000000000  0.2602536969696985
  0.2488012914285349  0.9999981545456791  0.3111025824177105
  0.2498114601995525  0.4999949000427790  0.3668296601323391
  0.0000000000000000  0.0000000000000000  0.1575786969696935
  0.0000000000000000  0.5000000000000000  0.2089156969696973
  0.0000000000000000  0.0000000000000000  0.2602536969696985
  0.0000010457235504  0.4999978932520506  0.3127698398941448
  0.0000010228279805  0.9999974060824286  0.3631599784468023
  0.7500000000000000  0.5000000000000000  0.1575786969696935
  0.7500000000000000  0.0000000000000000  0.2089156969696973
  0.7500000000000000  0.5000000000000000  0.2602536969696985
  0.7512025463223821  0.9999965942390503  0.3111026604081175
  0.7501904299772590  0.4999945671723225  0.3668303978292045
  0.5000000000000000  0.0000000000000000  0.1575786969696935
  0.5000000000000000  0.5000000000000000  0.2089156969696973
  0.5000000000000000  0.0000000000000000  0.2602536969696985
  0.5000015639031119  0.4999964591729054  0.3126721337741927
  0.4999996805913227  0.9999940548666615  0.3614400574329366
  0.2500000000000000  0.1938200000000023  0.1575786969696935
  0.2500000000000000  0.6938200000000023  0.2089156969696973
  0.2500000000000000  0.1938200000000023  0.2602536969696985
  0.2498138188794030  0.6950934514968665  0.3119658044028313
  0.2524280138077089  0.1861127666091065  0.3669600310534236
  0.2500000000000000  0.8061799999999977  0.1575786969696935
  0.2500000000000000  0.3061799999999977  0.2089156969696973
  0.2500000000000000  0.8061799999999977  0.2602536969696985
  0.2498121211832114  0.3049036406056587  0.3119651440843825
```

286	0.2524266263582291	0.8138771097060129	0.3669582433245679
287	0.0000000000000000	0.5000000000000000	0.1376786969696937
288	0.0000000000000000	0.0000000000000000	0.1890156969696974
289	0.0000000000000000	0.5000000000000000	0.2403536969696987
290	0.0000033366723002	0.9999983995869286	0.2916725552676525
291	0.9999983919523387	0.4999903140637088	0.3443788620816264
292	0.0000000000000000	0.0000000000000000	0.1261406969696992
293	0.0000000000000000	0.5000000000000000	0.1774786969697004
294	0.0000000000000000	0.0000000000000000	0.2288156969696971
295	0.0000000000000000	0.5000000000000000	0.2801536969696983
296	0.0000004702753174	0.0000010749354971	0.3322192919898654
297	0.0000024779424166	0.4999976716803474	0.3850642866602882
298	0.7500000000000000	0.1938200000000023	0.1575786969696935
299	0.7500000000000000	0.6938200000000023	0.2089156969696973
300	0.7500000000000000	0.1938200000000023	0.2602536969696985
301	0.7501895022306897	0.6950943052876610	0.3119655807604360
302	0.7475722175676367	0.1861129237780830	0.3669596767773555
303	0.7500000000000000	0.8061799999999977	0.1575786969696935
304	0.7500000000000000	0.3061799999999977	0.2089156969696973
305	0.7500000000000000	0.8061799999999977	0.2602536969696985
306	0.7501888836023696	0.3049013558887452	0.3119649427430957
307	0.7475750105729020	0.8138756194580452	0.3669583389013908
308	0.5000000000000000	0.5000000000000000	0.1376786969696937
309	0.5000000000000000	0.0000000000000000	0.1890156969696974
310	0.5000000000000000	0.5000000000000000	0.2403536969696987
311	0.5000004380020968	0.9999981878708368	0.2916762329082587
312	0.5000031242622427	0.4999898338493480	0.3443024431194672
313	0.5000000000000000	0.0000000000000000	0.1261406969696992
314	0.5000000000000000	0.5000000000000000	0.1774786969697004
315	0.5000000000000000	0.0000000000000000	0.2288156969696971
316	0.5000000000000000	0.5000000000000000	0.2801536969696983
317	0.5000012013600355	0.9999999986327168	0.3313422089567268
318	0.4999992045790762	0.5000003464454466	0.3851619919671947
319	0.0000250963547970	0.4999936477690170	0.4683204433035613
320	0.0000004323464040	0.5000028999194015	0.5667833635182475
321	0.0000000000000000	0.4999970000000005	0.6656369999999967
322	0.0000000000000000	0.4999970000000005	0.7624050000000011
323	0.5000163581316812	0.0000144177316841	0.4273653299013915
324	0.4999971217290877	0.9999649589003567	0.5225504840442738
325	0.4999960349328916	0.9999463868439449	0.6178962161364936
326	0.5000000000000000	0.9999970000000005	0.7140210000000025
327	0.5000000000000000	0.9999970000000005	0.8107880000000023
328	0.9999970827007587	0.0000313764720730	0.4187342643481600
329	0.0000002820529019	0.9999913632752211	0.5215388593159318

```
0.9999992153274349 0.9998499468851918 0.6174694162594960
0.0000000000000000 0.9999970000000005 0.7140210000000025
0.0000000000000000 0.9999970000000005 0.8107880000000023
0.5000009837753439 0.4999865760275455 0.4355208878590844
0.5000055981173972 0.4999935062842695 0.5230460129512622
0.5000006892508821 0.4999092907060287 0.6175328757073970
0.5000000000000000 0.4999970000000005 0.7140210000000025
0.5000000000000000 0.4999970000000005 0.8107880000000023
0.4999980781488631 0.9999854088675804 0.4732069177875218
0.5000006557914958 0.9999737545646994 0.5696037908008762
0.5000000000000000 0.9999970000000005 0.6656369999999967
0.5000000000000000 0.9999970000000005 0.7624050000000011
0.9645370000000000 0.8547900000000013 0.1215946969696944
0.6489130000000003 0.0328710000000001 0.1212646969696962
0.4686540000000008 0.8537740000000014 0.1216146969696936
0.4971370000000022 0.3833580000000012 0.1272986969696959
0.1497930000000025 0.0292540000000017 0.1212716969696999
0.9970289999999977 0.3828060000000022 0.1273536969696991
```

3. POSCAR of the prototype-III heterojunction

```
System
  1.00000000000000
    6.4278000000000022    0.0000000000000000    0.0000000000000000
    0.0000000000000000    6.5815999999999999    0.0000000000000000
    0.0000000000000000    0.0000000000000000   66.0000000000000000
  Sn   O   Cs   Pb   I   H
  20   44   4    5   14   6
Selective dynamics
Direct
  0.2500000000000000 0.5000000000000000 0.1536087499999965
  0.2500000000000000 0.0000000000000000 0.2049462350000013
  0.2500000000000000 0.5000000000000000 0.2562837199999990
  0.2514810102489804 0.0010476725229793 0.3080321229219862
  0.2442230196552941 0.5055153413731261 0.3592188810646917
  0.0000000000000000 0.0000000000000000 0.1536087499999965
  0.0000000000000000 0.5000000000000000 0.2049462350000013
  0.0000000000000000 0.0000000000000000 0.2562837199999990
  0.0020442146920701 0.5020401000140993 0.3074588043911106
  0.0039018928030004 0.0027680168452875 0.3601006693609605
  0.7500000000000000 0.5000000000000000 0.1536087499999965
  0.7500000000000000 0.0000000000000000 0.2049462350000013
  0.7500000000000000 0.5000000000000000 0.2562837199999990
  0.7505811096865287 0.0012373610606957 0.3080515485282049
  0.7676417637444573 0.5038942690652704 0.3600576453774309
  0.5000000000000000 0.0000000000000000 0.1536087499999965
```

374	0.5000000000000000	0.5000000000000000	0.2049462350000013
375	0.5000000000000000	0.0000000000000000	0.2562837199999990
376	0.5025264815308148	0.5008316976206544	0.3080253353511964
377	0.5044920027690338	0.0079434599893915	0.3601818359637932
378	0.2500000000000000	0.1938200000000023	0.1536087499999965
379	0.2500000000000000	0.6938200000000023	0.2049462350000013
380	0.2500000000000000	0.1938200000000023	0.2562837199999990
381	0.2543312663587827	0.6943009204821635	0.3080127307354061
382	0.2500152103371533	0.1986047185936570	0.3599723389020255
383	0.2500000000000000	0.8061800000000048	0.1536087499999965
384	0.2500000000000000	0.3061799999999977	0.2049462350000013
385	0.2500000000000000	0.8061800000000048	0.2562837199999990
386	0.2532886568036616	0.3080028379030679	0.3082748558679782
387	0.2550663616715809	0.8118276286382127	0.3601424912221063
388	0.0000000000000000	0.5000000000000000	0.1337088874999992
389	0.0000000000000000	0.0000000000000000	0.1850463724999969
390	0.0000000000000000	0.5000000000000000	0.2363838575000017
391	0.0000000000000000	0.0000000000000000	0.2877213424999994
392	0.0030858949535073	0.5087651222541183	0.3384669273986418
393	0.0201202748742446	0.0066629088035057	0.3939278372945054
394	0.0000000000000000	0.0000000000000000	0.1221711275000033
395	0.0000000000000000	0.5000000000000000	0.1735086125000009
396	0.0000000000000000	0.0000000000000000	0.2248460974999986
397	0.0000000000000000	0.5000000000000000	0.2761835825000034
398	0.0021075700036306	0.9997586742578335	0.3282207649351463
399	0.0091835986026680	0.5035537212770578	0.3796293115478733
400	0.7500000000000000	0.1938200000000023	0.1536087499999965
401	0.7500000000000000	0.6938200000000023	0.2049462350000013
402	0.7500000000000000	0.1938200000000023	0.2562837199999990
403	0.7500882966300324	0.6946990511094882	0.3078521252403661
404	0.7582102205377481	0.1986951012217375	0.3589358027876841
405	0.7500000000000000	0.8061800000000048	0.1536087499999965
406	0.7500000000000000	0.3061799999999977	0.2049462350000013
407	0.7500000000000000	0.8061800000000048	0.2562837199999990
408	0.7511283311946357	0.3078249001362536	0.3080387426360076
409	0.7545399544518432	0.8105020097093956	0.3604707110907839
410	0.5000000000000000	0.5000000000000000	0.1337088874999992
411	0.5000000000000000	0.0000000000000000	0.1850463724999969
412	0.5000000000000000	0.5000000000000000	0.2363838575000017
413	0.5000000000000000	0.0000000000000000	0.2877213424999994
414	0.5069888216780143	0.5032391352646499	0.3409824067699958
415	0.5211983106275682	0.0278865313920846	0.3904587366996992
416	0.5000000000000000	0.0000000000000000	0.1221711275000033
417	0.5000000000000000	0.5000000000000000	0.1735086125000009

418	0.5000000000000000	0.0000000000000000	0.2248460974999986
419	0.5000000000000000	0.5000000000000000	0.2761835825000034
420	0.5018657308633934	0.0022387078327881	0.3283581747038582
421	0.4995277772094582	0.5076047447989112	0.3815801821520424
422	0.9900360271452513	0.5023570812399996	0.4868726268901540
423	0.9998859830896549	0.5002932036386198	0.5758963775816923
424	0.0000000000000000	0.4999969612252357	0.6656373236363677
425	0.0000000000000000	0.4999969612252357	0.7624047386363628
426	0.3116687838150369	0.0388089527926567	0.4146137527628397
427	0.5043580357414541	0.9957933966529211	0.5197341962624407
428	0.5000000000000000	0.9999969612252357	0.6172536161363666
429	0.5000000000000000	0.9999969612252357	0.7140210311363617
430	0.5000000000000000	0.9999969612252357	0.8107884461363639
431	0.8594053735478440	0.8177924721925862	0.4120994991595381
432	0.0040902371744380	0.9974089541208428	0.5226450012826191
433	0.0000000000000000	0.9999969612252357	0.6172536161363666
434	0.0000000000000000	0.9999969612252357	0.7140210311363617
435	0.0000000000000000	0.9999969612252357	0.8107884461363639
436	0.4432372839814747	0.5189204667623457	0.4107344496350152
437	0.4985167393187950	0.4963907942944772	0.5227657547431903
438	0.5000000000000000	0.4999969612252357	0.6172536161363666
439	0.5000000000000000	0.4999969612252357	0.7140210311363617
440	0.5000000000000000	0.4999969612252357	0.8107884461363639
441	0.5188250373955228	0.9905008835006939	0.4730695035678565
442	0.5030753985207284	0.9989178046770562	0.5699398415326584
443	0.5000000000000000	0.9999969612252357	0.6656373236363677
444	0.5000000000000000	0.9999969612252357	0.7624047386363628
445	0.9645374970829863	0.8547901037103429	0.1176249574090917
446	0.6489129522542711	0.0328708501686492	0.1172948860000034
447	0.4686543544447588	0.8537741083414332	0.1176448164772737
448	0.4971371328837222	0.3833582525829584	0.1233293035454537
449	0.1497928347957327	0.0292538666555231	0.1173024187500005
450	0.9970292443370994	0.3828062550990623	0.1233840871818188